Bound on Hot-Spot Mix in High-Velocity, High-Adiabat Direct-Drive Cryogenic Implosions Based on Comparison of Absolute X-Ray and Neutron Yields

R. C. Shah,[1] D. Cao,[1] L. Aghaian,[2] B. Bachmann,[2] R. Betti,[1] E. M. Campbell,[1] R. Epstein,[1] C. J. Forrest,[1] A. Forsman,[2] V. Yu. Glebov,[1] V. N. Goncharov,[1] V. Gopalaswamy,[1] D. R. Harding,[1] S. X. Hu,[1] I. V. Igumenshchev,[1] R. T. Janezic,[1] L. Keaty,[2] J. P. Knauer,[1] D. Kobs,[2] A. Lees,[1] O. M. Mannion,[1] Z. L. Mohamed,[1] D. Patel,[1] M. J. Rosenberg,[1] C. Stoeckl,[1] W. Theobald,[1] C. A. Thomas,[1] P. Volegov,[3] K. M. Woo,[1] and S. P. Regan[1]

[1]Laboratory for Laser Energetics, University of Rochester
[2]Lawrence Livermore National Laboratory
[3]Los Alamos National Laboratory

Here we report on new continuum x-ray measurements to characterize hot-spot x-ray yield and hot-spot electron temperature of a series of implosions typical of current best cryogenic designs.[1] The objective of these measurements is to consider the consistency of x-ray production relative to neutron production and assess if this ratio implies hot-spot mix. Because of the insufficient time for equilibration given plasma parameters in these high-velocity implosions, there are significant differences between the hot-spot electron and ion temperature, which can influence the comparison of the x-ray and neutron yields. Based on the measured neutron yield and both hot-spot temperatures, the expected x-ray yield (assuming a pure-DT hot spot) is determined for each implosion and then compared to the measured x-ray yield. The x-ray and neutron yields are found to be consistent without invoking hot-spot mix within an estimated sensitivity corresponding to ~2% by atom, fully ionized carbon–deuterium plastic.

The x-ray yield and electron-temperature measurements were newly developed for this experiment. Approximately 30 images of each implosion were generated using an array of differentially filtered circular apertures and recorded on an absolutely calibrated image plate (IP).[2] The imaging apertures make it possible to distinguish the hot-spot x rays from a background of neutrons and coronal x rays (the spatial identification of hot spot as compared to coronal x rays was corroborated with simulation data). The x rays were filtered with Al foils in order to have four data channels. After accounting for IP response, the mean recorded energies of the channels ranged from 10 to 18 keV. In this range, the dense fuel was optically thin, and the signal level was within the dynamic range of a single scan read of the IP (consistent with the calibration). The channel measurements were used to constrain an isobaric hot-spot model, and the hot spot (assumed static) was used to calculate the volume integrated bremsstrahlung x-ray continuum using the free–free emissivity for hydrogen. [Figures 1(a)–1(c) show examples of the data, measured and modeled channel signals, and inferred spectrum for shot 96806.] Finally, a neutron-weighted electron temperature (T_e) was calculated to parameterize the hot-spot electron temperature on similar footing as the ion temperature. For the simulations, post-processed x rays were spatially and temporally selected to isolate the hot-spot contribution. The hot-spot x rays from the simulations were then filtered by the experimentally used channel responses and analyzed using the same procedure as for the data.

The measured hot-spot electron and ion temperatures for five cryogenic implosions of 25 February 2020 that are typical of current best performing designs, as well as the values from 1-D simulation, are shown in the bar plot of Fig. 2. In contrast to the x-ray yield and electron temperature, neutron yield and ion temperature are routinely measured in inertial confinement fusion experiments on OMEGA. The hot-spot ion temperature (T_i) is inferred based on the temporal width of the neutron time of flight (nTOF), which, under ideal circumstances, characterizes a neutron-weighted ion temperature. This inferred T_i will be inflated by flows, which, if anisotropic, will result in variations of the inferred value as observed from different lines of sight.[3] In our experiments, there were five independent nTOF's and shown are the maximum and minimum values of T_i for each shot. The range between the extremes was large for only the first shot, for which a target defect was observed and believed to cause a large

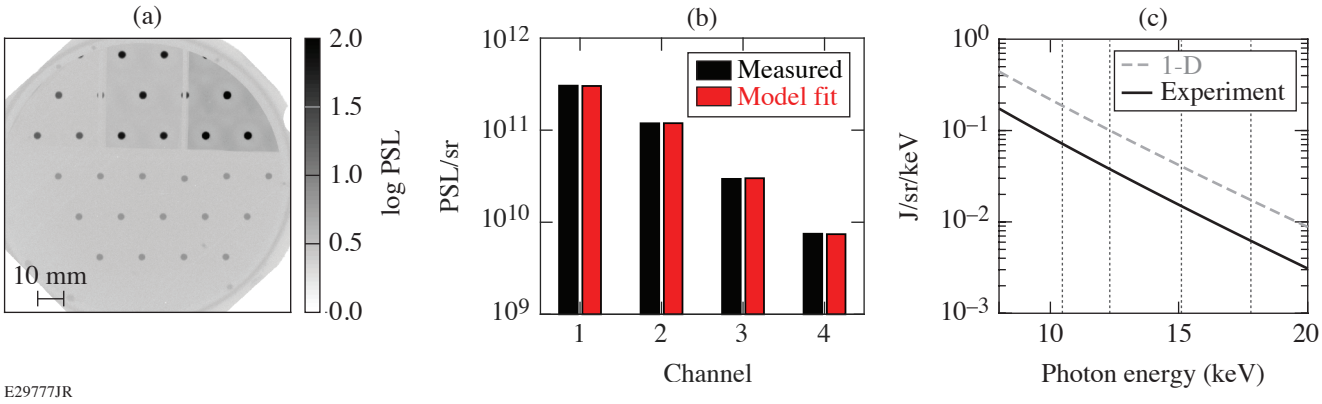

Figure 1
(a) Image-plate data for shot 96806 with image intensity reported in units of photostimulated luminescence (PSL). (b) Measured and fit channel signals. (c) The hot-spot model x-ray spectrum determined from the channel data. Dotted vertical lines indicate the mean recorded energy of each of the four imaging channels. For reference, the hot-spot model x-ray spectrum obtained from the identical analysis of the 1-D simulation is also plotted.

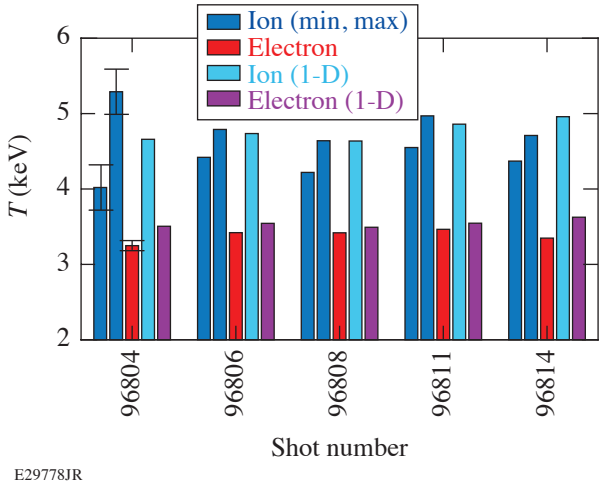

Figure 2
The measured hot-spot T_e is typically ~75% of the minimum T_i obtained from five independent lines of sight. The result is similar to what is obtained from 1-D simulations.

flow. In that case, the minimum T_i takes its lowest value. We have used the minimum nTOF T_i as the value best representative of the ion thermal conditions. Note that for the x-ray and neutron yield ratio comparison, an inflated value of T_i will increase the estimated hot-spot mix; therefore, in this sense the inferred mix quantification will be an upper bound estimate. Figure 2 also shows that the measured T_e value is typically ~75% of the minimum T_i. This degree of equilibration is similar to what is obtained in the 1-D simulation.

The predicted x-ray yield (Y_x) for a hot spot in the absence of mix is calculated using these temperatures as well as the measured neutron yield (Y_n). This result, along with the measured Y_x, is plotted in Fig. 3(a). There is a generally positive correlation of the measured x-ray and neutron yields contrasting what was reported by Ma *et al.*[4] in indirect-drive implosions of the National Ignition Campaign and for which mix was identified as a prominent issue. Additionally, since the measured and mapped values of Y_x do not significantly deviate, there is no measurable indication that mix is consistently present across these implosions. This is more explicitly shown in Fig. 3(b) as the ratio of the measured to mapped values, or x-ray enhancement. In this plot, the variability observed in the application of the model to a set of test simulations is indicated by the shaded region, and we interpret it as an estimate of the sensitivity by which we can measure an enhancement due to mix. The dashed lines in Fig. 3(b) indicate the value of the x-ray enhancement estimated for specified fractions of mix in the hot spot, accounting for the increase in both bremsstrahlung and recombination emission due to the carbon atoms. The measurement sensitivity is compromised by both the

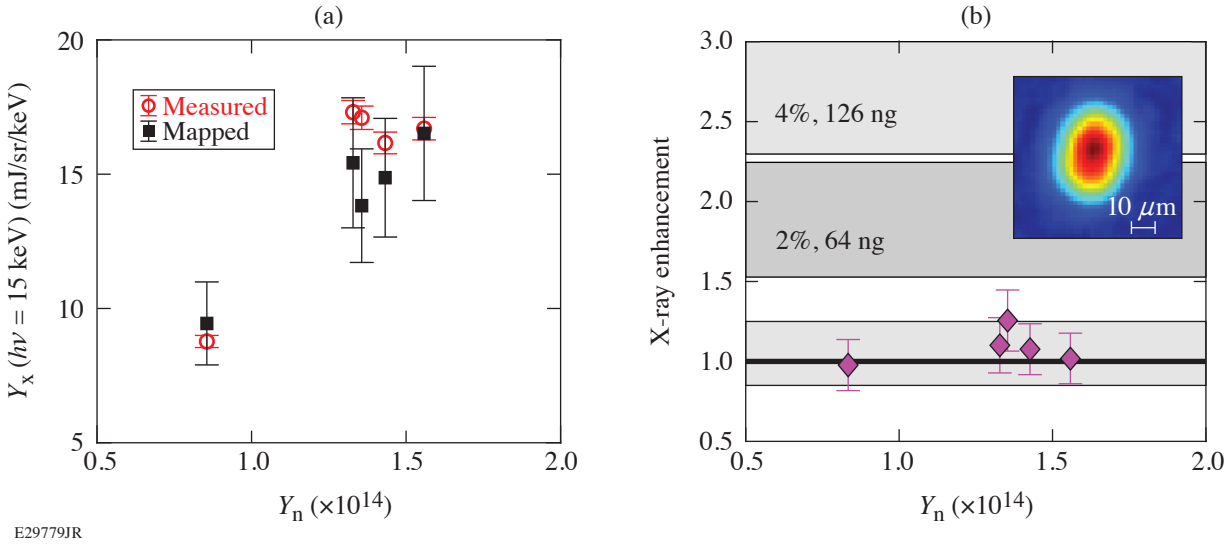

Figure 3
For each implosion, the measured Y_n, T_i, and T_e are used to calculate a mapped x-ray yield that is compared to the measured x-ray yield. (b) The x-ray enhancements fall within the systematic errors observed for the mapping (as determined by tests on a simulation database) indicated by the shaded gray region of the plot. The percentage values refer to percent-by-atom levels of CD mix required to cause the indicated level of x-ray enhancement. The inset shows the recovered hot-spot image from channel 1 for shot 96806.

error propagation (dominated by the hot-spot temperatures and indicated with error bars) as well as the model errors (indicated by the shaded region). We find no indication of hot-spot mix within the combined effect of these errors or an approximate sensitivity limited to ~2% by atom carbon–deuterium (64 ng, assuming a typical 1.2-μg hot spot). We have also extracted the hot-spot images from image-plate data using an established approximation to tomographic analysis,[5,6] applicable to the precisely machined circular apertures (General Atomics, San Diego). The inset of Fig. 3(b) shows the image with an estimated 8-μm resolution obtained from channel 1 for shot 96806. Typical of all the implosion and other channels, we do not identify the sorts of bright features which have been associated with mix in other experiments[7] in hot-spot images of these and similar implosions. It is plausible that decompression, peripheral bubbles, and residual motions, observed in multidimensional simulations[8] and also previously proposed based on experimental signatures,[9] dominate the hydrodynamic degradations without creating hot-spot mix.

In summary, measurements were presented of the x-ray yield and hot-spot electron temperature for direct-drive cryogenic implosion experiments. The comparison of the electron temperature with the ion temperature routinely characterized in the experiments was consistent with the prediction that ions and electrons remain substantially unequilibrated in the high-velocity, high-adiabat designs of present interest. The independently measured electron and ion temperatures of the hot spot with the D–T fusion neutron yield were used to estimate a corresponding x-ray yield expected from the nonequilibrium DT hot spot, assuming the absence of mix. The comparison of the measured and expected x-ray yields is consistent within the estimated sensitivity of the technique and therefore indicates that hot-spot mix, if present in these implosions, is at levels less than what the yield comparison can detect.

This material is based upon work supported by the Department of Energy National Nuclear Security Administration under Award Number DE-NA0003856, the University of Rochester, and the New York State Energy Research and Development Authority.

1. V. Gopalaswamy *et al.*, Nature **565**, 581 (2019).
2. M. J. Rosenberg *et al.*, Rev. Sci. Instrum. **90**, 013506 (2019); 029902(E) (2019).
3. T. J. Murphy, R. E. Chrien, and K. A. Klare, Rev. Sci. Instrum. **68**, 610 (1997).
4. T. Ma *et al.*, Phys. Rev. Lett. **111**, 085004 (2013).
5. B. Bachmann *et al.*, Rev. Sci. Instrum. **87**, 11E201 (2016).
6. G. Di Domenico *et al.*, Med. Phys. **43**, 294 (2016).

7. A. Pak *et al.*, Phys. Rev. Lett. **124**, 145001 (2020).
8. D. Cao *et al.*, "Understanding Origins of Observed Fusion Yield Dependencies," to be submitted to Physical Review Letters.
9. A. Bose *et al.*, Phys. Rev. E **94**, 011201(R) (2016).